Aus dem Institut für Transfusionsmedizin
der Medizinischen Fakultät Charité – Universitätsmedizin Berlin

DISSERTATION

Investigation of interactions between biopolymer submicron particles and tumour cells carrying albumin receptors

zur Erlangung des akademischen Grades
Doctor rerum medicinalium (Dr. rer. medic.)

vorgelegt der Medizinischen Fakultät
Charité – Universitätsmedizin Berlin

von

Saranya Chaiwaree

aus Chiang Mai (Thailand)

Datum der Promotion: 04.06.2021

Table of Contents

Abstrakt (Deutsch)

Biopolymere dienen in der Medizin u.a. als Drug Carrier aufgrund ihrer Biokompatibilität, Bioabbaubarkeit, hohen Stabilität und ihrer Fähigkeit verschiedene Arzneimittel reversibel zu binden. In der AG-Bäumler (Charité) wurde ein neuartiges Verfahren zur Herstellung von Biopolymerpartikeln im Submikrogrößenbereich entwickelt, welches unter der Bezeichnung CCD-Technik publiziert wurde. CCD steht für Copräzipitation-Crosslinking-Dissolution. Das Verfahren liefert Proteinpartikel mit homogener Morphologie und einer engen Größenverteilung. In diese Partikel können Arzneimittel, Vitamine, Nanopartikel (NP) und Enzyme eingeschlossen werden. Sowohl die Einschlusseffizienz als auch die Freisetzung der eingeschlossenen Moleküle und/oder NPs hängt sowohl vom Biopolymer als auch von der einzuschließenden Substanz ab. In dieser Arbeit werden hauptsächlich Eigenschaften von Humanserumalbumin Partikel (HSA-MP) beladen mit Doxorubicin (DOX) untersucht. Es wurden die Größen, Zetapotential, Morphologie, Einschlusseffizienz und Freisetzung von Doxorubicin bestimmt. Die Einschlusseffizienz von Doxorubicin betrug bezogen auf die Ausgangsmenge 25,6 ± 1,1 %. Außerdem wurde die Wechselwirkung von DOX-HSA-MPs mit Lungenkarzinomzellen A549 sowie menschlichen bronchialen Epithelzellen (BEAS-2B) untersucht, da die A549-Zellen Albuminrezeptoren exprimieren, während die BEAS-2B-Zellen keine derartigen Rezeptoren besitzen. Damit sollte die Hypothese geprüft werden, dass die DOX-HSA-MP das Wachstum der Tumorzellen verringern, während das Wachstum der Epithelzellen unbeeinflusst bleibt. Es konnte gezeigt werden, dass die DOX-HSA-MP von den Tumorzellen endozytiert und im Lysosom abgebaut werden, wodurch das gebundene Doxorubicin freigesetzt und die metabolische Aktivität der A549-Tumorzellen nach 72h Inkubation um 60% verringert wird.

Abstract (English)

Biopolymers are used in medicine, among other things, as a drug carrier due to their biocompatibility, biodegradability, high stability and ability to bind various drugs reversibly. At AG-Bäumler (Charité), a novel procedure for the fabrication of biopolymer particles in the submicron range was developed and published under the name CCD technology. CCD stands for co-precipitation–crosslinking-dissolution. This method delivers protein particles with a homogeneous morphology and a narrow size distribution. Drugs, vitamins, nanoparticles (NP) and enzymes can be included in these particles. Both the entrapment efficiency and the release of the enclosed molecules and / or NPs depend on the biopolymer used and, on the substance to be enclosed. In this work, mainly properties of human serum albumin particles (HSA-MP) loaded with doxorubicin (DOX) are investigated. The size, zeta potential, morphology of particles as well as the entrapment efficiency and release of doxorubicin were determined. The entrapment efficiency of DOX was 25.6 ± 1.1% from the initially applied amount of the drug. The interaction of DOX-loaded HSA-MP (DOX-HSA-MPs) with human lung carcinoma cells A549 expressing albumin receptors and non-cancerous human bronchial epithelial cells (BEAS-2B) without these receptors was also investigated. The aim of these experiments was to test the hypothesis that the DOX-HSA-MP reduce the growth of the tumor cells while the growth of the non-cancerous epithelial cells remains unaffected. It could be shown that the DOX-HSA-MP are endocytosed by the tumor cells and broken down in the lysosome, whereby the bound doxorubicin is released and the metabolic activity of the A549 tumor cells is reduced by 60% after 72h.

1.Introduction

The production of nano / microparticles using biopolymers has found increasing use for biomedical applications. It has established itself as a promising class of materials with good biocompatibility, biodegradation and non-cytotoxicity (e.g. albumin, and polyelectrolyte complex dispersions (PEC) [1–3]. These properties can make biopolymers an excellent candidate for materials for use in biomedical applications.

Albumin is a natural biopolymer and is suitable for particle fabrication because of its good biocompatibility, biodegradability, low toxic, and non-immunogenic properties [4,5] Albumin is the most abundant plasma protein that is used for biodistribution molecules in the body and accounts for 60% of the total plasma protein content [6,7]. This protein can be bound with therapeutic hydrophobic and hydrophilic drugs to form stable complexes [8–10] Furthermore, human serum albumin (HSA) has been more attractive for using in drug delivery system due to its solubility, stability to pH changes (pH between 4 to 9) [11], modifying the distribution of drugs in tissues and the ability to improve intracellular distribution [12,13]. The natural transport function and cellular interactions provide a rational basis for the use of albumin for drug delivery [14].

Recently, a technique was developed at the Charité which allows the fabrication of biopolymer particles known as Co-precipitation Crosslinking Dissolution technique (CCD-technique) [15–20]. During the formation of micro or submicro-carbonate particles, the biopolymers are trapped in these particles (co-precipitation). The biopolymers are then intermolecularly crosslinked within the insoluble inorganic matrix with the help of aldehydes. Finally, the carbonate templates were dissolved using EDTA to obtain the biopolymer particles.

The biopolymer particles, which fabricated from CCD-technique, showed an uniform peanut-like shape with a narrow distribution between 700 and 1000 nm and negative zeta-potential. However, the particle size and shape can be controlled by adjusting the experimental conditions (e.g. pH, choice of salt and/or salt concentration, temperature, rate of mixing the solutions)[18]. In particularly, the carbonate particles not only can be loaded with bioactive compounds (e.g. hemoglobin and albumin) during their formation but also entrapped drug and vitamin into porous of carbonate template.

Doxorubicin is one of the most effective drugs to treat several types of cancer such as lung or breast cancer. Two major mechanisms are under discussion to explain its cytotoxic effect: intercalating into DNA leading to DNA synthesis inhibition; and generation of free radicals leading to DNA and cell damage [21–23]. DOX is also known to be cardiotoxic [24] and its clinical application is limited by detrimental effect on normal tissues including brain, kidney, liver [25,26] and skin [27] . Furthermore, as conventional chemotherapeutic drug DOX exhibits high toxicity due to the limited accessibility of the drug by the tumor cell. To avoid these effects, various types of drug carriers have been developed. Currently, pegylated liposomal doxorubicin (Doxil®, Lipodox®) and non-pegylated (Myocet®) (FDA-approved) [28], encapsulated dextran–DOX conjugate using chitosan nanoparticles [29], DOX-loaded mesoporous silica nanoparticle [30] and DOX-encapsulated in micelles or nano-emulsion [31] are being investigated as possible candidates.

In recent years, albumin has been actively explored and considered as a reliable and efficient carrier for drug delivery systems [4,5,32] , because many tumor cells express albumin receptors [8] and therefor crucial for the cellular uptake of albumin particles. The receptor-associated albumin-binding proteins have been discovered such as albondin/glycoprotein 60 (gp60), glycoprotein 18 (gp18), glycoprotein 30 (gp30), a secreted protein acidic and rich in cysteine (SPARC) and the neonatal Fc receptor (FcRn) [33–35]. Furthermore, a number of receptor-associated albumin-binding proteins have been identified in various tissues and cell lines including kidney, endothelium, fibroblasts and tumor cell surfaces. Interestingly, the existence of albumin receptors (albondin) has been demonstrated for the A549 human lung adenocarcinoma cell line. Albondin (gp60) is a 60 kDa glycoprotein, which not only specifically binds native albumin, but also facilitates its internalization and subsequent transcytosis [36]. This study aims to investigate the interactions of our synthesized biopolymer particles with human lung tumour cell line (A549) and with human bronchial epithelia cells (BEAS-2B).

2.Material and Methods

2.1 Material

Table 1: List of all substances

Substances	**Abbreviation**	**Company**
Doxorubicin	DOX	Cayman Chemical
Glutaraldehyde	GA	Sigma-Aldrich
Manganese chloride tetrahydrate	$MnCl_2 \cdot 4H_2O$	Sigma-Aldrich
Sodium carbonate	Na_2CO_3	Sigma-Aldrich
Glycine	$C_2H_5NO_2$	Sigma-Aldrich
Sodium borohydride	$NaBH_4$	Sigma-Aldrich
10x Phosphate buffered saline pH 7.4	PBS	Fisher Scientific
20% Human albumin solution	HSA	Grifols Deutschland GmbH
Sodium hydroxide	NaOH	Carl Roth
Dimethyl sulfoxide	DMSO	Carl Roth
Ampuwa® (aqua ad injectable)	-	Fresenius Kabi
0.9% Sodium chloride	NaCl	Fresenius Kabi
RPMI 1640		Corning
Bronchial Epithelial Basal Medium	BEBM	Lonza
Test kits		
CCK-8 Cell counting kit		Dojindo EU GmbH
Lysotracker Deep Red		Invitrogen
Cell line		
Human lung adenocarcinoma cell line	A549	ATCC
Human normal bronchial epithelium cell line	BEAS-2B	Sigma-Aldrich

Table 2: List of equipment/facility

Equipment/facility	**Company**
Hematocrit centrifuge	Mikro 22R, Hettich GmbH & CoKG, Tuttlingen, Germany
Confocal laser scanning microscopy	CLSM ZeissLSM 510 meta, Zeiss MicroImaging GmbH, Jena, Germany
Atomic force microscopy	Digital Instrument Inc., Santa Barbara, CA, USA
Atomic force microscopy	Bruker, Berlin, Germany
Scanning Electron Microscope (SEM)	LV-Scanning Electron Microscope, JSM 5910 LV, Tokyo, Japan
Flow cytometry	FACS-Canto II, Becton and Dickinson, Franklin Lakes City, NJ, USA.
Magnetic Stirrer	Bibby Scientific CB161, Bibby Sterilin Ltd., Stone, Staffordshire, UK.
Zetasizer nano instrument	Malvern Instruments Ltd., Malvern, UK
Nanoscope III Multimode AFM	Digital Instrument Inc., Santa Barbara, CA, USA
PowerWave340 Microplate reader	BioTek Instruments GmbH, Bad Friedrichshall, Germany

2.2 Particles Fabrication using CCD-technique

Two types of particles HSA-MP and HbMP were produced. HSA-MP were loaded either with DOX or with RF, the HbMP were loaded with polydopamine. Here we focus on the DOX-HSA-MP and will not describe details of the fabrication of RF-HSA-MP or Dopamin-HbMP. Details are given in the attached papers [20][37].

2.2.1 HSA-MPs

The HSA-MPs were fabricated using a modification of a previously described CCD-technique [15,16]. Briefly, 20 mL of 0.5 M $MnCl_2$ solution containing 10 mg/mL HSA were mixed in a beaker for 1 min. Then 20 mL of 0.25 M Na_2CO_3 were added rapidly under vigorous stirring at room temperature (RT). The obtained hybrid particles were separated by centrifugation and washed twice with 0.9% NaCl solution. The particles were incubated in a GA solution (final concentration 0.1%) at RT for 1 h. After

centrifugation, 0.08 M glycine and 0.625 mg/mL $NaBH_4$ were added to quench the remaining unbound aldehyde groups of GA in the particles. Subsequently, the $MnCO_3$ template was removed by treatment with EDTA solution (0.25 M, pH 7.4) at RT for 30 min. Finally, the resulting particles were centrifuged, washed 3 times and resuspended in sterile 0.9% NaCl for further use.

2.2.2 DOX-HSA-MPs

Equal volumes of 0.125 M of $MnCl_2$ containing 0.5% HSA of 0.125 M of Na_2CO_3 were mixed rapidly for 30 s under vigorous stirring using a magnetic stirrer at room temperature. Then, 0.05 % of HSA solution was added to the suspension and incubated for further 5 min under stirring to prevent agglomeration of the particles. The suspension was centrifuged and the particles were washed 2 times (3,000×g for 3 min). The resulting particle suspension was adjusted to a volume concentration of 30 % and incubated with 10 mg/mL DOX in 50% DMSO for 1 h. After the incubation, the supernatant was collected and the particles were washed with 0.9% NaCl (3,000×g for 3 min) until the supernatant became colourless. The resulting particles (30 % volume concentration) were incubated with 0.1% GA solution for 1 h at an ambient temperature allowing the cross-linking reaction to perform in the formulated submicron particles. The remaining unbound GA were quenched by incubation with 0.08 M glycine and 0.625 mg/mL $NaBH_4$ for 30 min. The dissolution of $MnCO_3$ templates was performed by incubation with 0.5 M of EDTA at room temperature for 30 min. The obtained DOX-loaded HSA particles (DOX-HSA-MPs) were centrifuged, washed three times (10,000×g for 10 min) and finally suspended in sterile 0.9% NaCl.

2.3 Particles Characterization

2.3.1 Particle Size and Zeta-potential

The hydrodynamic diameter and the zeta-potential of all MPs were measured by dynamic light scattering using a Zetasizer Nano ZS instrument. Each sample was diluted 1:200 using PBS and all measurements were carried out in triplicate.

2.3.2 Scanning Electron Microscopy (SEM)

DOX-HSA-MPs and HSA-MPs were observed by SEM (LV-Scanning Electron Microscope, JSM 5910 LV, Tokyo, Japan). The samples were prepared by applying a

drop of the particle suspension on a glass slide and then dried overnight at room temperature. Afterward, the samples were sputtered and coated with gold. The images were conducted at an operation voltage of 15 kV.

2.3.4 Atomic Force Microscopy (AFM)

AFM investigations of DOX-HSA-MPs were performed using a NanoWizard®4 Bruker (Berlin, Germany). The samples were diluted in water and spread on a clean coverslip. The drop was completely dried after incubation at 30° C for 1 h and thereafter the cover slide was stored in dry conditions (air) for 4 days at 24° C. The images of the particles were then taken (dry state). For the wet stage images the clean cover slip was covered with poly-l-ornithine, rinsed with water and dried by nitrogen flow. The samples were dropped on the coverslip and incubated for 30 min. Afterwards the samples were thoroughly washed and imaged in water. The JPK Data Processing software (version 6.1, Bruker Nano GmbH, Berlin, Germany) was used to analyze the obtained images.

2.3.5 Confocal Laser Scanning Microscopy (CLSM)

CLSM images of HSA-MPs and DOX-HSA-MPs were taken with a confocal microscope LSM 510 Meta (Carl Zeiss Micro Imaging GmbH, Jena, Germany) equipped with 100× oil immersion objective (numerical aperture 1.3) Images of autofluorescence of HSA-MPs and intrinsic DOX-fluorescence in DOX-HSA-MPs were taken using excitation wavelength 488 nm (Ar laser) and a long pass filter 505 nm. Cells additionally stained with Lysotracker® Deep Red were imaged using excitation wavelength 633nm (HeNe laser) and emission long pass filter 650 nm. For intracellular co-localization of DOX-HSA-MPs and Lysotracker®Deep Red the particle fluorescence was detected using a band pass filter 530–600 nm.

2.3.6 Entrapment Efficiency

The amount of entrapped doxorubicin in DOX-HSA-MPs was calculated as the difference between the total applied doxorubicin amount (DOX_t) and the doxorubicin amount determined in the supernatant after absorption and after each washing step (ΣDOX_f). The entrapment efficiency EE % was calculated according to the following equation: $EE\ \% = (DOX_t - \Sigma DOX_f) \times 100\% / DOX_t$. The absorbance was measured with a microplate reader (PowerWave 340, BioTek Instruments GmbH) at 480 nm.

2.4 In vitro cell studies

2.4.1 Cytotoxicity

In vitro colorimetric determination of cytotoxicity was assessed using Cell Counting Kit 8 (CCK-8). This assay kit measures the metabolic activity of dehydrogenases within the viable cells and offers the viable percentage subjected to varying particles concentrations.

The A549 and BEAS-2B cells line were incubated for 24 h to allow them to adhere. After this period, HSA-MPs and DOX-HSA-MPs were added to the cells at concentrations of 1000; 5000 and 10,000 particles/cell. For control, the cells were incubated with cell culture media for 24, 48 and 72 h at 37^{o} C, 5% CO_2. Following these incubation times 10 µL of CCK-8 solution was added to each well and the plates were placed in the incubator for 1 h. Then the metabolic activity of the cells was assessed measuring the optical density at 450 nm using a microplate reader (PowerWave 340, BioTek Instruments GmbH)

The mean absorbance of the control cells at 24 h was set to 100% and used as a reference value. Afterward, statistical evaluation of data was performed using an analysis of variance (two-way ANOVA). Tukey's multiple comparisons were used to compare the significance of the difference in each sample. A value of $p < 0.05$ was considered statistically significant.

2.4.2 Cellular uptake of HSA-MPs and DOX-HSA-MPs

To investigate the uptake of particles, A549 cells were plated at a density $1x10^5$ cells/well in 24-well cell culture plates and incubated in a 5% CO_2 humidified incubator at 37° C for 24 h. The particle suspensions (1,000 and 5,000 particles/cell) were then added and incubated for 24 h. Following an incubation time, the cells were washed and fixed with PBS and 4% paraformaldehyde, respectively. Percentage of cells with an uptake of particles was determined by flow cytometer (BD FACS-Canto II, BD Biosciences, NJ) and CLSM.

2.4.3 Intracellular Colocalization

A549 cells were plated at a density $1x10^5$ cells/well in 24-well plate and incubated in a 5% CO_2 humidified incubator at 37° C for 24 h. The particle suspensions (5,000 particles/well) was added and incubated for 24 h. 30 min before the end of

incubation, 50 nM Lysotracker® Deep Red was added into the wells. After that, cells were washed and fixed with PBS and 4% paraformaldehyde, respectively.

3. Results

3.1 Fabrication and Characterisation of Biopolymer submicron Particles

We have successfully fabricated DOX-HSA-MPs via a modified CCD-technique. DOX is absorbed within the porous structure of the $MnCO_3$-HSA-MPs. Meanwhile, the albumin and adsorbed DOX are crosslinked with glutaraldehyde. Finally, the $MnCO_3$ template is dissolved with EDTA and the final DOX-HSA-MPs are obtained.

3.1.1 The particles size and Zeta potential

The particle size and zeta-potential of HSA-MPs and DOX-HSA-MPs measured by dynamic light scattering were submicron size (around 700-1000 nm). The zeta potential HSA-MPs and DOX-HSA-MPs measured in PBS were not significantly different (-13 mV ± 0.8 mV, conductivity 18-20 mS/cm)

3.1.2 Morphology

The morphology of HSA-MPs and modified HSA-MPs was analyzed using an AFM image. The shape of HSA-MPs and DOX-HSA-MPs was peanut-like. Figure 1 shows images of AFM measurements illustrating the topography and size of particles in both dry and wet state and HSA-MPs in three dimensional (3D)-mode. These measurements provide highly accurate determination of the particle dimensions and deliver additional information about the topography of their surface. The high-resolution AFM topography images also show the peanut-like shape of particles with submicron size and rough structures on the surface. The particles size was further determined under two different conditions. (i) In the dry state, HSA-MPs and DOX-HSA-MPs were in the same size range: length 690±50 nm and a height 480±40 nm. (ii) In the wet state, the size range of HSA MPs as well as of DOX-HSA-MPs was 950±60 nm (length) and 615±20 nm (height). The size increase in the wet state is due to the swelling of MPs and their sponge like behavior.

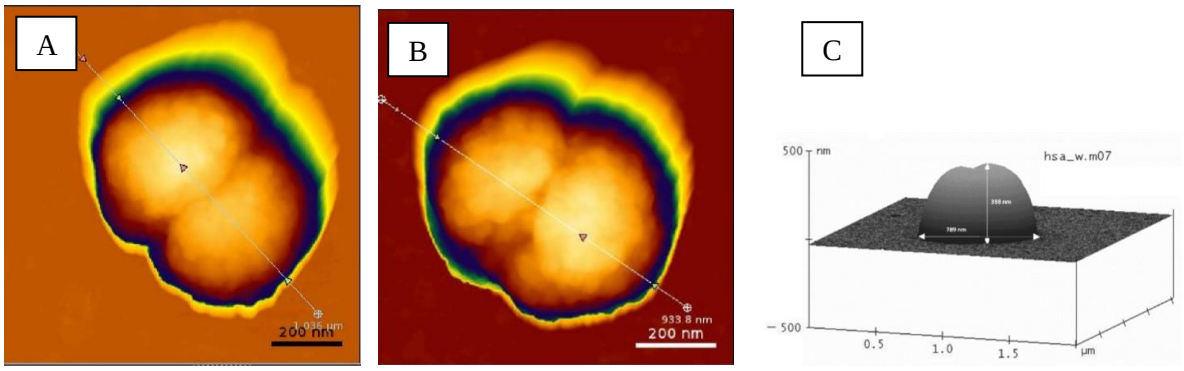

Figure 1 Atomic force microscopy images of (A) HSA-MPs and (B) DOX-HSA-MPs particles in the dry state and (C) HSA particles (HSA-MPs) in three dimensional (3D)-mode.

3.1.3 Entrapment efficiency

A high drug entrapment in drug carriers not only reduces the clinical dose required, but also the toxic side effects of the system and improves the therapeutic effect [34,36]. To achieve the highest possible DOX concentration in the particles, doxorubicin hydrochloride was dissolved in 50% (v/v) DMSO in water and added to concentrated particle suspension (30% v/v). The entrapment efficiency for doxorubicin under these conditions was 25±1.5% which corresponds to 7.25 fg DOX per particle.

3.2 Invitro cell studies

3.2.1 Metabolic activity and Cytotoxicity in A549 and BEAS-2B cell line

The A549 cell line has been widely used as a model system for the development of drug therapies against lung cancer. The cytotoxicity of HSA-MPs and DOX-HSA-MPs was examined by determining their effects on the mitochondrial metabolic activity of the cells after 24, 48 and 72 h exposure. At the lower particle concentrations (1000 and 5000 particles per cell), no significant differences between the metabolic activity of the cells cultured with both types of particles and that of the untreated cells were found. However, after 72 h exposure to the highest particle concentration of 10,000 particles per cell the cell metabolic activity in the group treated with DOX-HSA-MPs was significantly decreased. Remarkably, the effect on the A549 cells caused by the DOX-HSA-MPs containing a total DOX dose of 0.725 µg/mL (72 pg/cell, related to the seeded cell number) was almost the same as that was achieved by 1 µg/mL (100 pg/cell, related to the seeded cell number) free DOX added to the cell culture medium. However, free DOX reduced the metabolic activity significantly already after 48 h treat-

ment. The faster effect of free DOX was expectable in the context, that the time-consuming uptake of the particles and their digestion by the cells were necessary to release the drug.

In parallel, the DOX-HSA-MPs were also cultured with the non-cancerous cell line BEAS-2B derived from normal human bronchial epithelium. Here, also 1000, 5000 and 10,000 particles were added per seeded cell. The CCK-8 assay resulted in no significant differences between the cells cultured with DOX-HSA-MPs and untreated cells (Figure 2).

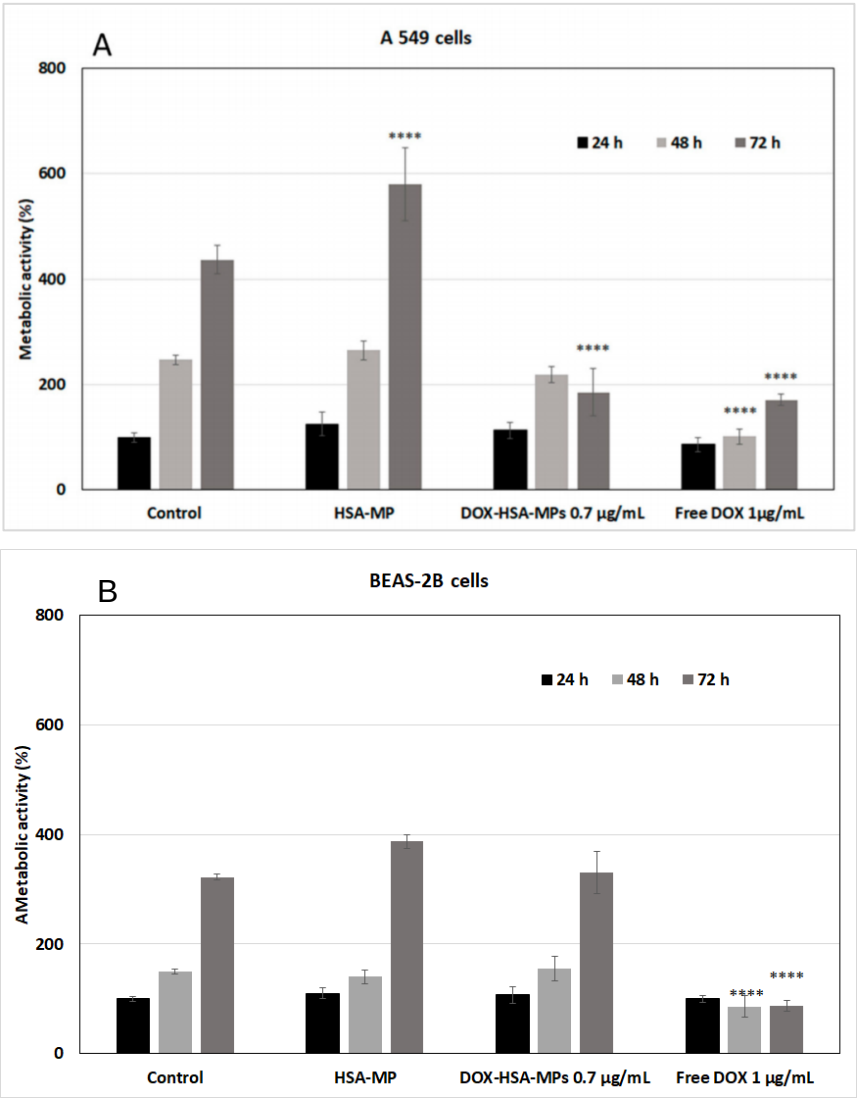

Figure 2 Metabolic activity of A549 lung tumor cells (A) and BEAS-2B bronchial epithelial cells (B) treated with HSA-MPs, DOX-HSA-MPs (10,000 particles per cell, corresponding to 0.725 µg/mL DOX) and free DOX (1µg/mL) for 24,48 and 72 h compared to untreated cells (control) using the Cell Counting Kit-8 (CCK-8) assay. The data are represented as two way ANOVA, Tukey's multiple comparisons. The error bar represents mean±SD; ****p < 0.001. The metabolic activity of the control after 24h was taken as 100%.

3.2.2 Cellular Uptake of HSA-MPs and DOX-HSA-MPs

For the quantitative determination of the cellular uptake of HSA-MPs and DOX-HSA-MPs we applied flow cytometry. As already observed by CLSM, both types of particles can be visualized by their intrinsic fluorescence if excited at 488 nm. For flow cytometry, we applied the APC channel in order to avoid influences by intrinsic fluorescence of the cells, which possibly can occur after their fixation with formaldehyde and is more intense if excited with wavelengths in the blue range. In order to clearly demonstrate the cellular uptake, we first determined the mean fluorescence intensity and distribution of the fluorescence intensity inside the particle populations (Figure 3). It can be seen that the DOX-HSA-MPs have a stronger fluorescence with a maximum over 1500 a.u. The HSA-MPs have a very weak fluorescence with a maximum around 500 a.u.

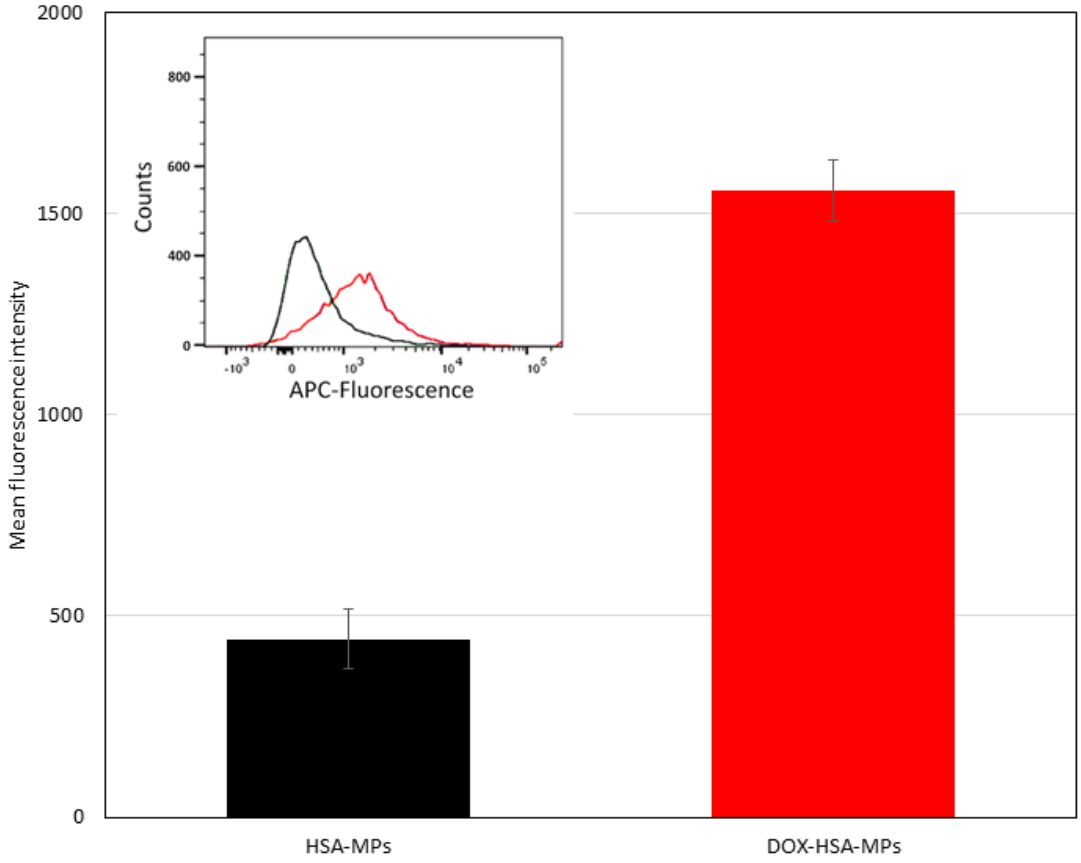

Figure 3 Mean fluorescent intensity (MFI) of HSA-MPs and DOX-HSA-MPs in the Allophycocyanin (APC) channel. Insert: Flowcytometry histograms showing the APC-fluorescence intensity distribution of the two types of particles (black line—HSA-MPs; red line—DOX-HSA-MPs).

Figure 4 summarizes the results of the cellular uptake experiments performed by incubating A549 cells with the particles in two different concentrations (1000 and 5000 particles/cell) for 24 h. At the lower particle concentration, the percentage of cells with uptake of HSA-MPs and DOX-HSA-MPs was 10.3% and 21.7%, respectively. At the higher particle concentration, the percentage of cells with uptake of DOX-HSA-MPs was increased more than 3-fold (69.5%), whereas the cells with uptake of HSA-MPs was only doubled (21%).

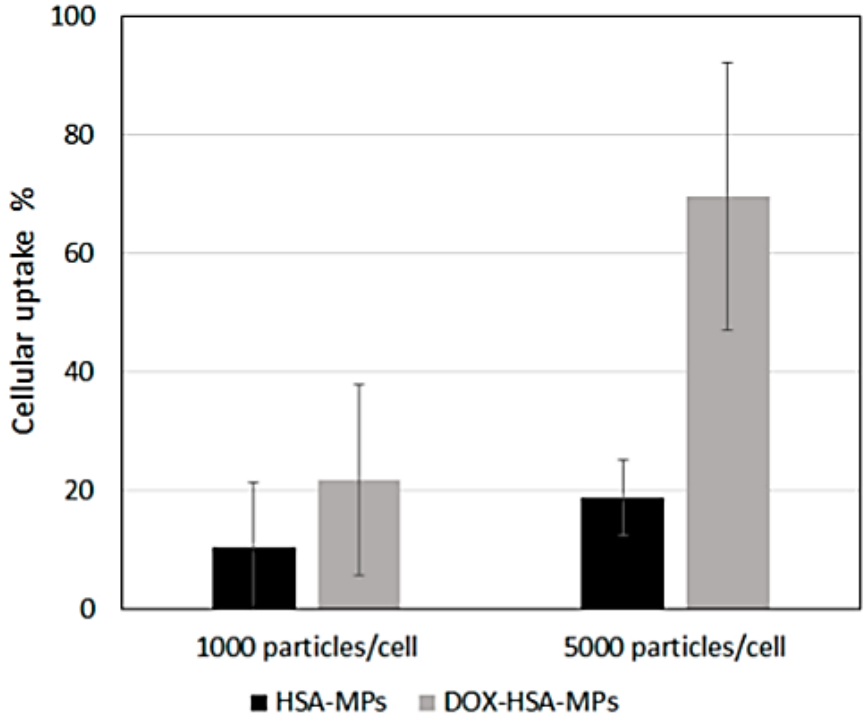

Figure 4 Cellular uptake of HSA-MPs and DOX-HSA-MPs (1000 and 5000 particles/cell) by A549 cells after culturing for 24 h.

To determine the location of particles in the cell compartments, A549 and BEAS-2B cells were incubated with DOX-HSA-MPs (5000 particles/cell) for 24 h and studied by CLSM. Figure 5 shows representative images of both samples. Obviously, BEAS-2B cells do not interact with the particles. A large number of DOX-HSA-MPs is distributed around the cell and close to the cell surface but inside the cells there are almost no particles (Figure 5, upper panel). The images of the A549 cells incubated with DOX-HSA MPs demonstrate a strong uptake (Figure 5, lower panel) with almost no particles in the space outside the cells, which corresponds to the results obtained by flow cytometry, presented above.

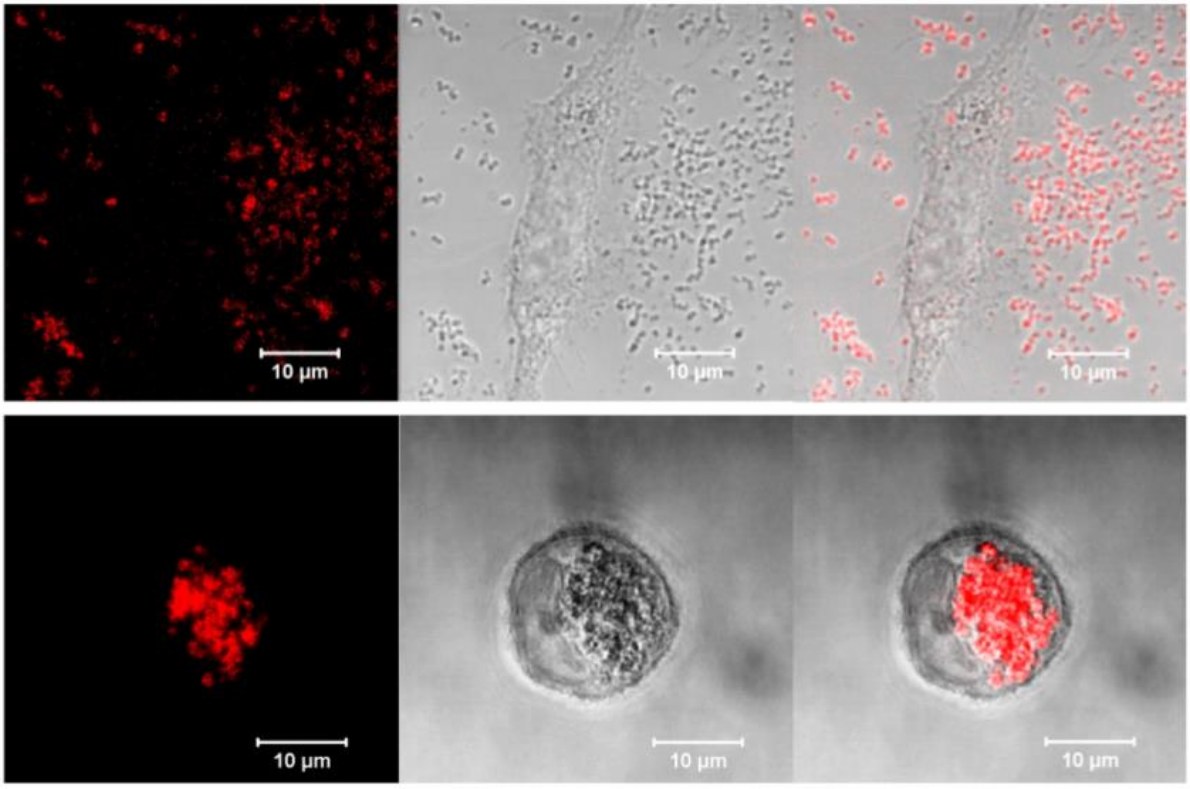

Figure 5 Representative CLSM images in fluorescence, transmission and overlay modes of a Beas-2B cell (upper panel) and an A549 cell (lower panel) after 24 h culturing with DOX-HSA-MPs (5000 particles per cell). Fluorescence mode was accessed with excitation of DOX at 488 nm and long pass emission filter 530 nm.

3.3.3 Intracellular Colocalization

The localisation of the particles after their endocytoses was investigated in the experiments. The A549 cells were additionally labelled with Lysotracker® Deep Red, a lysosomal marker. After incubation for 24 h with 5000 particles per cell the samples were studied by CLSM. A representative image is shown in Figure 6.

The lower imaged cell has internalized two DOX-HSA-MPs. The upper cell is out of focus. The overlapping of the red (DOX) and blue (Lysotracker® Deep Red) colour confirms co-localization of both fluorophores and therefore the co-localization of particles and lysosomes. This localization is important for the degradation of the particles by lysosomal enzymes and for the release of the drug from the degraded particles.

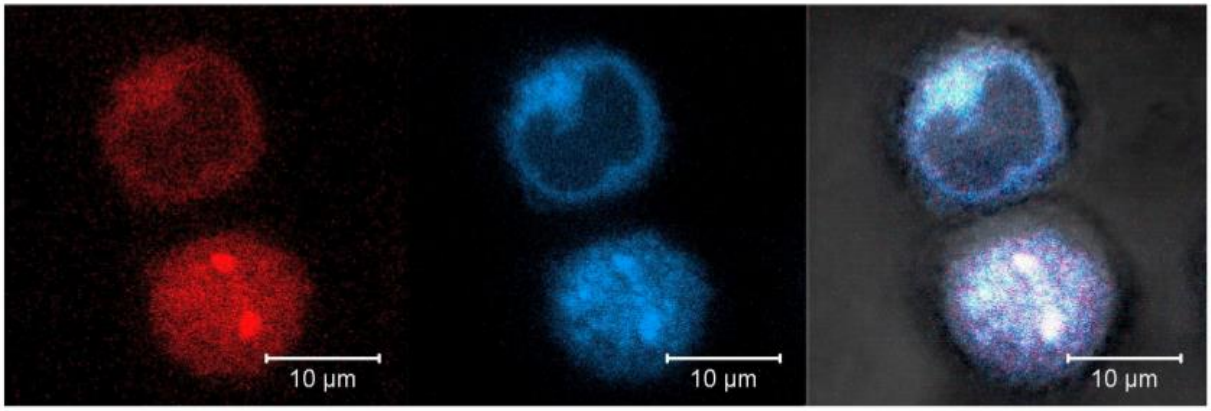

Figure 6 Representative CLSM images in fluorescence, transmission and overlay modes of A549 cells after 24 h culturing with DOX-HSA-MPs (5000 particles/cell) and Lysotracker® Deep Red staining. Fluorescence modes was accessed with excitation at 488 nm and band pass emission filter 530/600 nm for DOX (red color) and excitation at 633 nm and long pass emission filter 650 nm for Lysotracker® Deep Red (blue color).

4. Discussion

The specific delivery of therapeutic agents to an organ, a tissue or a type of cells is currently a major challenge for the treatment of human diseases. The use of nanotechnology in medicine today enables the concept of drug targeting to be realized. We successful fabricated the biopolymer submicron particles fabricated based on the CCD-technique, which captured the protein and other molecules during the precipitation process. This procedure provided the uniform peanut-like shape morphology, monodisperse and submicron size range particles.

To fabricate DOX-HSA-MPs, DOX was adsorbed within the $MnCO_3$-HSA-MPs and bound to albumin due to the porous structure of the MPs. After crosslinking of HSA within the $MnCO_3$ template, the $MnCO_3$ template was dissolved with EDTA and the final DOX-HSA-MPs were obtained. $MnCO_3$-MPs as template have a high adsorption capacity for biomolecules due to electrostatic interactions. Moreover, during the adsorption step, DOX can bind strongly to HSA via hydrophilic, hydrophobic contacts and hydrogen bond [7,33,38]. Additionally, during the crosslinking with glutaraldehyde covalent cross-bounds are formed between amino groups of neighboring albumin molecules but also between albumin and adsorbed DOX which also contains an amino group[39]. Finally, the $MnCO_3$ template is dissolved with EDTA and the final DOX-HSA-MPs are obtained.

The entrapment efficiency for doxorubicin was 25.57±1.12 % which corresponds to 7.25 fg DOX per particles. A high drug entrapment efficiency in drug carriers does not only reduce the necessary clinical dose, but also decreases the toxic side effects of the system and improves the therapeutic effect [34,38]. Doxorubicin hydrochloride, the salt form of DOX, improves the solubility of DOX in water, but DOX itself showed good solubility in DMSO. However, high concentrations of DMSO disturbed protein binding [40], which must be taken into account when DOX is adsorbed in HSA-MPs.

The cytotoxicity of HSA-MPs and DOX-HSA-MPs was examined by determining their effects on the mitochondrial metabolic activity of the cells after 24, 48 and 72 h exposure. The endocytoses of HSA-MPs by tumor cells, results in an increase of the metabolic activity in comparison with that of the untreated cells. HSA-MPs consist of albumin, which is known to have an impact on the metabolic activity, cell proliferation and survival of cells by an interaction with such as co-factors, hormones, growth factors, lipids, amino acids, metal ions, reactive oxygen and nitrogen species [35]. This could be understood as an extra nutrition for the cells.

In case of the DOX-HSA-MPs, the digestion of MPs in the lysosome where more than 60 different types of enzymes [41] are included leads to the release of DOX which interferes with the DNA [36]. After digestion DOX and other breakdown products are released into the cytoplasm compartment. DOX generates free radicals which interfere and damage the cellular membranes, DNA and proteins of the cells finally resulting in cell death [42]. Therefore, the cells metabolic activity decreases at lower dose than after free DOX after treatment.

Our results are in concordance with a previous report about Abraxane (Abr), which is an albumin nanoparticle-bound Paclitaxel (PTX), a chemotherapy agent [43]. It has been highlighted that Abr exhibited a greater effect for the treatment of non-small-cell lung cancer compared to free PTX. The authors found that albumin down regulates the protein glucosamine6-phosphateN-acetyltransferase1(GNA1) causing proliferative delay and cell adhesion defects in A549 cells and leading to the superior drug effect of Abr.

The A549 cells incubated with DOX-HSA-MPs demonstrate a strong uptake with almost no particles in the space outside the cells. whereas, BEAS-2B cells do not

interact with the particles. This could be demonstrated that albumin is a promising drug delivery vehicle and it can pass into the A549 cells via binding to its receptors [14,44]. This characteristic allows DOX-HSA-MPs to pass into cancer cell while, no interaction of DOX-HSA-MPs were found when the particles were cultured with non-albumin receptors cell line BEAS-2B.

For the mean fluorescence intensity and distribution of the fluorescence intensity inside the particle populations. The DOX-HSA-MPs showed a stronger fluorescence intensity inside the particle than those in the HSA-MPs. It can be explained by the inherent fluorescence of DOX associated with its central anthracycline chromophore group which entrapped in the particles [45]. This factor makes the quantitative determination of their uptake by the cells difficult. The cellular uptake experiments were found to be tremendously influenced by fluorescence intensity inside the particles. DOX-HSA-MPs showed a strong uptake over 3 times than HSA-MPs. Due to the significantly lower mean fluorescence intensity of the HSA-MPs the uncertainty of the obtained values is high and it is not possible to claim that the DOX-HSA-MPs are preferably internalized by the A549 cells.

Intracellular localization experiment confirmed that DOX-HSA-MPs are internalized into the lysosome of A549 cell line. This localization is important for the degradation of the particles by lysosomal enzymes. The possible pathway of the proteolytic degradation and intracellular localization of DOX-HSA-MPs is the particles are firstly taken up at cell surface via endocytosis. Then, lysosomes and endosomes fuse to form autolysosomes and the scavenged particles are digested by lysosomal enzymes. After digestion DOX and other breakdown products are released into the cytoplasm compartment. DOX generates free radicals which interfere and damage the cellular membranes, DNA and proteins of the cells finally resulting in cell death.

We have successfully loaded DOX into protein particles via CCD technique. The DOX-HSA-MPs exhibited a submicron size with negative zeta potential. The DOX entrapped into protein particles around 25% which is likely due to hydrophilic, hydrophobic contacts and hydrogen bond between DOX and albumin in the $MnCO_3$ template. The DOX-HSA-MPs showed higher efficacy inhibiting the metabolic activity of A549 cells at lower dose than free DOX after treatment for 3 days, which correlated well with their localization in the lysosomal compartment. In addition, no uptake and toxic effects

of DOX-HSA-MPs were found when the particles were cultured with the non-cancerous cell line BEAS-2B. This demonstrates that our carriers are a highly promising drug delivery system for an alternative chemotherapy treatment of cancer.

5. References

[1] Nitta, S. K.; Numata, K. Biopolymer-Based Nanoparticles for Drug / Gene Delivery and Tissue Engineering. *Int. J. Mol. Sci*. **2013**, 1629–1654.

[2] Elzoghby, A. O.; Samy, W. M.; Elgindy, N. A. Albumin-Based Nanoparticles as Potential Controlled Release Drug Delivery Systems. *J. Control. Release* **2012**, *157* (2), 168–182.

[3] Hartig, S. M.; Greene, R. R.; Carlesso, G.; Higginbotham, J. N.; Khan, W. N.; Prokop, A.; Davidson, J. M. Kinetic Analysis of Nanoparticulate Polyelectrolyte Complex Interactions with Endothelial Cells. *Biomaterials* **2007**, *28* (26), 3843–3855.

[4] Cantin, A. M.; Paquette, B.; Richter, M.; Larivée, P. Albumin-Mediated Regulation of Cellular Glutathione and Nuclear Factor Kappa B Activation. *Am.J.Respir.Crit. Care Med.* **2000**, *162* (4 I), 1539–1546.

[5] Koziol, M. J.; Sievers, T. K.; Smuda, K.; Xiong, Y.; Müller, A.; Wojcik, F.; Steffen, A.; Dathe, M.; Georgieva, R.; Bäumler, H. Kinetics and Efficiency of a Methyl-Carboxylated 5-Fluorouracil-Bovine Serum Albumin Adduct for Targeted Delivery.*Macromol.Biosci.* **2014**, *14* (3),428–439.

[6] Wang, R. E.; Tian, L.; Chang, Y. H. A Homogeneous Fluorescent Sensor for Human Serum Albumin. *J. Pharm. Biomed. Anal.* **2012**, *63*, 165–169.

[7] Gun'ko, V. M.; Turov, V. V.; Krupska, T. V.; Tsapko, M. D. Interactions of Human Serum Albumin with Doxorubicin in Different Media. *Chem. Phys.* **2017**, *483–484*, 26–34.

[8] Lomis, N.; Westfall, S.; Farahdel, L.; Malhotra, M.; Shum-Tim, D.; Prakash, S. Human Serum Albumin Nanoparticles for Use in Cancer Drug Delivery:Process Optimization and In Vitro Characterization. *Nanomaterials* **2016**, *6* (6), 116.

[9] Yang, F.; Zhang, Y.; Liang, H. Interactive Association of Drugs Binding to Human Serum Albumin. *Int. J. Mol. Sci*. **2014**, 3580–3595.

[10] Horv, B.; Simon, M.; Schwarz, C. M. Serum Albumin as a Local Therapeutic Agent in Cell Therapy and Tissue Engineering. *BioFactors*. **1980**, 1–16.

[11] Svedberg,T.; Sjogren, B. The Ph-Stability Regions of Serum Albumin and of Serum Globulin. *J. Am. Chem. Soc.* **1930**, *52* (7), 2855–2863.

[12] Bae, S.; Ma, K.; Kim, T. H.; Lee, E. S.; Oh, K. T.; Park, E. S.; Lee, K. C.; Youn, Y. S. Doxorubicin-Loaded Human Serum Albumin Nanoparticles Surface-Modified with TNF-Related Apoptosis-Inducing Ligand and Transferrin for Targeting Multiple Tumor Types. *Biomaterials* **2012**, *33* (5), 1536–1546.

[13] Geller, D. M.; Judah, J. D.; Nicholls, M. R. Intracellular Distribution of Serum Albumin and Its Possible Precursors in Rat Liver. *Biochem. J.* **2015**, *127* (5), 865–874.

[14] Wang, S.; Liu, S.; He, J.; David, H.Human Serum Albumin (HSA) and Its Applications as a Drug Delivery Vehicle Abstract. *Heal. Sci J* **2020**, *14* (14:2),1–8.

[15] Bäumler, H.; Georgieva, R. Coupled Enzyme Reactions in Multicompartment Microparticles. *Biomacromolecules* **2010**, *11* (6), 1480–1487.

[16] Xiong, Y.; Steffen, A.; Andreas, K.; Muller, S.; Sternberg, N.; Georgieva, R. Hemoglobin-Based Oxygen Carrier Microparticles: Synthesis, Properties, and In Vitro and In Vivo Investigations. *Biomacromolecules*. **2012**. 13, 3292− 3300

[17] Bäumler, H.; Xiong, Y.; Liu, Z. Z.; Patzak, A.; Georgieva, R. Novel Hemoglobin Particles-Promising New-Generation Hemoglobin-Based Oxygen Carriers. *Artif. Organs* **2014**, *38* (8), 708–714.

[18] Xiong, Y.; Georgieva, R.; Steffen, A.; Smuda, K.; Bäumler, H. Structure and Properties of Hybrid Biopolymer Particles Fabricated by Co-Precipitation Cross-Linking Dissolution Procedure. *J. Colloid Interface Sci.* **2018**, *514*, 156–164.

[19] Kao, I.; Xiong, Y.; Steffen, A.; Smuda, K.; Zhao, L.; Georgieva, R.; Pruss, A.; Bäumler, H. Preclinical In Vitro Safety Investigations of Submicron Sized Hemoglobin Based Oxygen Carrier HbMP-700. *Artif. Organs* **2018**, 42 (5), 549–559

[20] Suwannasom, N.; Smuda, K.; Kloypan, C.; Kaewprayoon, W.; Baisaeng, N.; Prapan, A.; Chaiwaree, S.; Georgieva, R.; Bäumler, H. Albumin Submicron Particles with Entrapped Riboflavin—Fabrication and Characterization. *Nanomaterials* **2019**, *9* (3), 482.

[21] Thorn, C. F.; Oshiro, C.; Marsh, S.; Hernandez-Boussard, T.; McLeod, H.; Klein, T. E.; Altman, R. B. Doxorubicin Pathways. *Pharmacogenet. Genomics* **2010**, *21* (7), 440–446.

[22] Taymaz-Nikerel, H.; Karabekmez, M. E.; Eraslan, S.; Kırdar, B. Doxorubicin Induces an Extensive Transcriptional and Metabolic Rewiring in Yeast Cells. *Sci. Rep.* **2018**, *8* (1), 1–14.

[23] Gruber, B. M.; Anuszewska, E. L.; Priebe, W. The Effect of New Anthracycline Derivatives on the Induction of Apoptotic Processes in Human Neoplastic Cells. *Folia Histochem. Cytobiol.* **2004**, *42* (2), 127–130.

[24] Octavia, Y.; Tocchetti, C. G.; Gabrielson, K. L.; Janssens, S.; Crijns, H. J.; Moens, A. L. Doxorubicin-Induced Cardiomyopathy: From Molecular Mechanisms to Therapeutic Strategies. *J. Mol. Cell. Cardiol.* **2012**, *52* (6), 1213–1225.

[25] Carvalho, C.; Santos, R.; Cardoso, S.; Correia, S.; Oliveira, P.; Santos, M.; Moreira, P. Doxorubicin: The Good, the Bad and the Ugly Effect. *Curr. Med. Chem.* **2009**, *16* (25), 3267–3285.

[26] Tangpong, J.; Miriyala, S.; Noel, T.; Sinthupibulyakit, C.; Jungsuwadee, P.; Clair, D. K. S. Doxorubicin-Induced Central Nervous System Toxicity and Protection by Xanthone Derivative of Garcinia Mangostana. *Neuroscience* **2011**, *175*, 292–299.

[27] Haas, R. L. M.; de Klerk, G. An Illustrated Case of Doxorubicin-Induced Radiation Recall Dermatitis and a Review of the Literature. *Neth. J. Med.* **2011**, *69* (2), 72–75.

[28] Kubicka-Wołkowska, J.; Kędzierska, M.; Lisik-Habib, M.; Potemski, P. Skin Toxicity in a Patient with Ovarian Cancer Treated with Pegylated Liposomal Doxorubicin: A Case Report and Review of the Literature. *Oncol. Lett.* **2016**, *12* (6), 5332–5334.

[29] Mitra, S.; Gaur, U.; Ghosh, P. C.; Maitra, A. N. *Tumour Targeted Delivery of Encapsulated Dextran-Doxorubicin Conjugate Using Chitosan Nanoparticles as Carrier*. *J Control Release*. **2001**, 74, 317-323.

[30] Yuan, Z.; Pan, Y.; Cheng, R.; Sheng, L.; Wu, W.; Pan, G.; Feng, Q.; Cui, W. Doxorubicin-Loaded Mesoporous Silica Nanoparticle Composite Nanofibers for Long-Term Adjustments of Tumor Apoptosis. *Nanotechnology* **2016**, *27* (24).

[31] Mohan, P.; Raporopt, N. Doxorubicin as a Molecular Nanotheranostic Agent: Effect of Doxorubicin Encapsulation in Micelles or Nanoemulsions on the Ultrasound-Mediated Intracellular Delivery and Nuclear Trafficking. *Mol Pharm* **2010**, *7* (30), 3921–3932.

[32] Zhang, L.; Cai, Q. Y.; Cai, Z. X.; Fang, Y.; Zheng, C. S.; Wang, L. L.; Lin, S.; Chen, D. X.; Peng, J. Interactions of Bovine Serum Albumin with Anti-Cancer Compounds Using a ProteOn XPR36 Array Biosensor and Molecular Docking. *Molecules* **2016**, *21* (12), 1–9.

[33] Collins, S. J.; Goldsmith, H. T. Spectral Properties of Fluorescence Induced by Glutaraldehyde Fixation. *J. Histochem. Cytochem.* **1981**, *29* (3), 411–414.

[34] Din, F.U.; Aman, W.; Ullah, I.; Qureshi, O.S.; Mustapha, O.; Shafique, S.Z.A. Effective Use of Nanocarriers as Drug Delivery Systems for the Treatment of Selected Tumors. *Int. J. Nanomed*. **2017,** 12, 7291–7309.

[35] Francis, G. L. Albumin and Mammalian Cell Culture: Implications for Biotechnology Applications. *Cytotechnology* **2010**, *62* (1), 1–16.

[36] Halim, V. A.; García-Santisteban, I.; Warmerdam, D. O.; van den Broek, B.; Heck, A. J. R.; Mohammed, S.; Medema, R. H. Doxorubicin-Induced DNA Damage Causes Extensive Ubiquitination of Ribosomal Proteins Associated with a Decrease in Protein Translation. *Mol. Cell. Proteomics* **2018**, *17* (12), 2297–2308.

[37] Baidukova, O.; Wang, Q.; Chaiwaree, S.; Freyer, D.; Prapan, A.; Georgieva, R.; Zhao, L.; Bäumler, H. Antioxidative Protection of Haemoglobin Microparti-cles (HbMPs) by PolyDopamine. *Artif. Cells, Nanomedicine Biotechnol.* **2018**, *46* (sup3), S693–S701.

[38] Liu, D.; Yang, F.; Xiong, F.; Gu, N. The Smart Drug Delivery System and Its Clinical Potential. *Theranostics*. **2016**, *6* (9), 1306–1323.

[39] Salem, M.; Mauguen, Y.; Prangé, T. Revisiting Glutaraldehyde Cross-Linking: The Case of the Arg-Lys Intermolecular Doublet. *Acta Crystallogr. Sect. F Struct. Biol. Cryst. Commun.* **2010**, *66* (3), 225–228.

[40] Tjernberg, A.; Markova, N.; Griffiths, W. J.; Hallén, D. DMSO-Related Effects in Protein Characterization. *J. Biomol. Screen.* **2006**, *11* (2), 131–137.

[41] Lübke, T.; Lobel, P.; Sleat, D. E. Proteomics of the Lysosome. *Biochim. Biophys. Acta - Mol. Cell Res.* **2009**, *1793* (4), 625–635.

[42] Yang, F.; Teves, S. S.; Kemp, C. J.; Henikoff, S. Doxorubicin, DNA Torsion, and Chromatin Dynamics. *Biochim. Biophys. Acta - Rev. Cancer* **2014**, *1845* (1), 84–89.

[43] Zhao, M. Z.; Li, H. Y.; Ma, Y.; Gong, H.; Yang, S.; Fang, Q.; Hu, Z. Y. Nanoparticle Abraxane Possesses Impaired Proliferation in A549 Cells Due to the Underexpression of Glucosamine 6-Phosphate N-Acetyltransferase 1 (GNPNAT1/GNA1). *Int. J. Nanomedicine* **2017**, *12*, 1685–1697.

[44] Peng, S. W.; Ko, W. H.; Yeh, M. K.; Chiang, C. H.; Chen, J. L. The Mechanism of High Transfection Efficiency of Human Serum Albumin Conjugated Polyethylenimine in A549 Cells. *J. Med. Sci.* **2015**, 35 (2), 57-61.

[45] Shankaranarayanan, J. S.; Kanwar, J. R.; Al-juhaishi, A. J. A.; Kanwar, R. K. Doxorubicin Conjugated to Immunomodulatory Anticancer Lactoferrin Displays Improved Cytotoxicity Overcoming Prostate Cancer Chemo Resistance and Inhibits Tumour Development in TRAMP Mice. *Scientific Report* .**2016**, 6, 32062.

Eidesstattliche Versicherung (Affidavit)

„Ich, Saranya Chaiwaree, versichere an Eides statt durch meine eigenhändige Unterschrift, dass ich die vorgelegte Dissertation mit dem Thema: Investigation of interactions between biopolymer submicron particles and tumour cells carrying albumin receptors selbstständig und ohne nicht offengelegte Hilfe Dritter verfasst und keine anderen als die angegebenen Quellen und Hilfsmittel genutzt habe.

Alle Stellen, die wörtlich oder dem Sinne nach auf Publikationen oder Vorträgen anderer Autoren beruhen, sind als solche in korrekter Zitierung kenntlich gemacht. Die Abschnitte zu Methodik (insbesondere praktische Arbeiten, Laborbestimmungen, statistische Aufarbeitung) und Resultaten (insbesondere Abbildungen, Graphiken und Tabellen werden von mir verantwortet.

Meine Anteile an etwaigen Publikationen zu dieser Dissertation entsprechen denen, die in der untenstehenden gemeinsamen Erklärung mit dem/der Betreuer/in, angegeben sind. Für sämtliche im Rahmen der Dissertation entstandenen Publikationen wurden die Richtlinien des ICMJE (International Committee of Medical Journal Editors; www.icmje.og) zur Autorenschaft eingehalten. Ich erkläre ferner, dass mir die Satzung der Charité – Universitätsmedizin Berlin zur Sicherung Guter Wissenschaftlicher Praxis bekannt ist und ich mich zur Einhaltung dieser Satzung verpflichte.

Die Bedeutung dieser eidesstattlichen Versicherung und die strafrechtlichen Folgen einer unwahren eidesstattlichen Versicherung (§156,161 des Strafgesetzbuches) sind mir bekannt und bewusst.“

_____

Datum Unterschrift

Anteilserklärung an den erfolgten Publikationen

Saranya Chaiwaree hatte folgenden Anteil an den aufgeführten Publikationen:

Publication 1: **Chaiwaree, S.;** Prapan, A.; Suwannasom, N.; Laporte, T.; Neumann, T; Pruß, A.; Georgieva, R.; Bäumler, H. Doxorubicin – Loaded Human Serum Albumin Submicron Particles: Preparation, Characterization and In Vitro Cellular Uptake. *Pharmaceutics*. **2020**, 12, 224.

IF 4.773 (2018)

Beitrag im Einzelnen:

Das Studiendesign wurde nach ausführlicher Literaturrecherche und Diskussion mit dem Supervisor festgelegt. Sie stellte die Mikropartikel nach dem sogenannten CCD-Verfahren (Copräzipitation, Crosslinking, Dissolution) her, belud die Mikropartikel mit Doxorubicin und charakterisierte sowohl die Morphologie als auch Einkapselungseffizienz der Partikel. In Zellkulturversuchen ermittelte sie die Wechselwirkung der Partikel mit Tumor- und Epithelzellen, insbesondere deren Endozytose und intrazelluläre Lokalisierung sowie die zytotoxische Wirksamkeit. Zur Partikelcharakterisierung und der Partikel-Zellwechselwirkung benutzte sie einen Zetasizer, ein Confokales Laserscanning Mikroskop, ein Durchflusszytometer sowie spektralphotometrische Messverfahren. Die Ergebnisse sind in den Abbildungen 1 bis 6 dargestellt.

Sie schrieb das Manuskript und diskutierte mit allen an der Publikation beteiligten Autoren die Methoden und Ergebnisse.

Publication 2: Suwannasom N.; Smuda K.; Kloypan C.; Kaewprayoon W.; Baisaeng N.; Prapan A.; **Chaiwaree S.;** Georgieva R.; Bäumler H. Albumin Submicron Particles with Entrapped Riboflavin—Fabrication and Characterization. *Nanomaterials*. **2019**, 9, 482.

IF= 4.034 (2018)

Beitrag im Einzelnen:

Auf der Grundlage des mit dem Supervisor festgelegten Studiendesigns führte S.C. insbesondere Untersuchungen zur Charakterisierung der mit Riboflavin beladenen Mikropartikel durch. Teilergebnisse sind in Abb. 1 dargestellt.

Publication 3: Baidukova, O.; Wang, Q.; **Chaiwaree, S.;** Freyer, D.; Prapan, A.; Georgieva, R.; Zhao, L.; Bäumler, H. Antioxidative protection of haemoglobin microparticles (HbMPs) by polydopamine. *Artif. Cells Nanomed. Biotechnol.* **2018**, *46*, S693–S701.

IF: 3.026 (2017)

In der Dissertation konnten nicht alle publizierten Ergebnisse dargestellt werden. S.C. Beitrag bei dieser Publikation bestand im folgenden:

Auf der Grundlage des mit dem Supervisor festgelegten Studiendesigns war S.C. sowohl bei der Herstellung der Partikel als auch bei den Untersuchungen der Zytotoxizität von Dopamin in den Zellkulturen beteiligt. Sie war an der Datensammlung, analyse und der Abfassung des Manuskripts beteiligt.

_____

Unterschrift, Datum und Stempel des betreuenden Hochschullehrers/der betreuenden Hochschullehrerin

_____

Unterschrift des Doktoranden/der Doktorandin

Printed copies of selected publications

1. Publication 1

Chaiwaree, S.; Prapan, A.; Suwannasom, N.; Laporte, T.; Neumann, T; Pruß, A.; Georgieva, R.; Bäumler, H. Doxorubicin – Loaded Human Serum Albumin Submicron Particles: Preparation, Characterization and In Vitro Cellular Uptake. Pharmaceitics. 2020; https://doi.org/10.3390/pharmaceutics12030224 **IF 4.773 (2018)**

2. Publication 2

Suwannasom N.; Smuda K.; Kloypan C.; Kaewprayoon W.; Baisaeng N.; Prapan A.; **Chaiwaree S.**; Georgieva R.; Bäumler H. Albumin Submicron Particles with Entrapped Riboflavin—Fabrication and Characterization. Nanomaterials. 2019;9(3):482. https://doi.org/10.3390/nano9030482 **IF= 4.034 (2018)**

3. Publication 3

Baidukova, O.; Wang, Q.; **Chaiwaree, S**.; Freyer, D.; Prapan, A.; Georgieva, R.; Zhao, L.; Baumler, H. Antioxidative protection of haemoglobin microparticles (HbMPs) by polydopamine. Artif. Cells Nanomed. Biotechnol. 2018, 46, S693–S701. https://doi.org/10.1080/21691401.2018.1505748 **IF: 3.026 (2017)**

Curriculum vitae

My CV is not included in the electronic version of the dissertation for data protection reasons.

Complete list of publications

Research articles

1. **Chaiwaree, S**.; Prapan, A.; Suwannasom, N.; Laporte, T.; Neumann, T; Pruß, A.; Georgieva, R.; Bäumler, H. Doxorubicin – Loaded Human Serum Albumin Submicron Particles: Preparation, Characterization and In Vitro Cellular Uptake. Pharmaceitics, 2020, 12, 224. **IF 4.773 (2018)**

2. Prapan, A.; Suwannasom, N.; Kloypan, C.; **Chaiwaree, S.**; Steffen, A.; Xiong, Y.; Kao,I.; Pruß, A.; Georgieva, R.; Bäumler, H. Surface Modification of Hemoglobin Based Oxygen Carriers Reduces the Recognition by Haptoglobin, Immunoglobulin and Hemoglobin Antibodies. Coat-ings, 2019, 9, 454. **IF: 2.330 (2018)**

3. Kloypan, C.; Prapan, A.; Suwannasom, N.; **Chaiwaree, S.**; Kaewprayoon, W.; Steffen, A.; Xiong, Y.; Georgieva, R.; Bäumler, H. Improved Oxygen Storage Capacity of Haemoglobin Submicron Particles by One-Pot Formulation. Artif. Cells Nanomed. Biotechnol. 2018, 46, S964-S972. **IF = 3.026 (2017)**

4. Baidukova, O.; Wang, Q.; **Chaiwaree, S.**; Freyer, D.; Prapan, A.; Georgieva, R.; Zhao, L.; Bäumler, H. Antioxidative Protection of Haemoglobin Microparticles (HbMPs) by Polydopamine. Artif. Cells Nanomed. Biotechnol. 2018, 46, S693-S701. **IF = 3.026 (2017)**

5. Kloypan, C.; Suwannasom, N.; **Chaiwaree, S**.; Prapan, A.; Smuda, K.; Baisaeng, N.; Pruß, A; Georgieva, R; Bäumler, H. In-vitro haemocompatibility of dextran-protein submicron particles. Artif. Cells Nanomed. Biotechnol. 2018, 47, 241-249. **IF= 3.026 (2017)**

6. Suwannasom, N.; Smuda, K.; Kloypan, C.; Kaewprayoon, W.; Baisaeng, N.; Prapan, A.; **Chaiwaree, S**.; Georgieva, R.; Bäumler, H. Albumin Submicron Particles with Entrapped Ribo-flavin—Fabrication and Characterization. Nanomaterials 2019, 9, 482. **IF= 4.034 (2018)**

Acknowledgement

I would like to express the deepest appreciation to **PD Dr. rer. nat. Hans Bäumler**, my supervisor, for providing me to join and work with AG-Bäumler I am thankful for his patience, motivation and encouragement knowledge. Without his guidance and persistent help this dissertation would not have been possible.

I would like to offer my special thanks to my co-supervisor, **Dr. rer. nat. Radostina Georgieva**, for her support, valuables suggestions and helpful comments for all of my papers.

I am also grateful for the continued interest and support of **Prof. Dr. Axel Pruß** in the progress of my work in the Institut für Transfusionsmedizin.

I particularly thank my labmates namely **Nittiya Suwannasom**, **Aussanai Prapan**, **Chirapat Kloypan**, **Waraporn Kaewprayoon**, **Quan Wang**, **Stefan Herrmann**, **Elena Rojas**, **Lamzira Ebralidze**, **Patcharin Thammasit** and **Kanyaluck Jantakee** for co-operation, stimulating discussions, mental support and all the enjoyment we had shared in the last three years of friendship.

I also thank scientists and technicians of AG-Bäumler including **Kathrin Smuda, Wanit Chaisorn**, **Axel Steffen, Yu Xiong, Josephine Waade, Anya Schnabel** who gave access to the laboratory and research facilities. Thanks for helping and good working atmosphere. In addition, I would like to express my special thanks to **Kathrin Smuda** (AG-Bäumler)**,** and **Pamela Glowacki** for solving the life problems and public affairs, making me live easily in Berlin.

My deep appreciation goes out to my former adviser, **Assoc.Prof.Dr.Yanee Pongpaibul** who had support throughout my study time in Germany.

This study might have never happened without the financial aid of support **Payap University**, Thailand.

Finally, I would like to express my wholehearted love to my father **"Somnit Chaiwaree"**, my mother **"Srila Chaiwaree"** my brother **"Nirun Chaiwaree"** and my close friend "**Benjawan Suksawat**", who had support throughout my study time in Germany. This accomplishment would not have been possible without them.